Comparison of Tribological Behavior of Single-Layer and Multilayer Electroless Nickel-Phosphorus Coatings in the Presence of Al_2O_3 and SiC Reinforcing Particles

A. I. Abduljaleel Al Rabeeah[1], M. Razazi Boroujeni[2,*]

[1]Department of Materials Engineering, South Tehran Branch, Islamic Azad University, Tehran, Iran.
[2]Department of Materials Engineering, Lenjan Branch, Islamic Azad University, Isfahan, Iran.
Received: 22 September 2023 - Accepted: 17 April 2024

Abstract

Due to their morphology, chemical composition, and phase structure, electroless nickel-phosphorus coatings are used on various substrates, including st37 steel, with the aim of improving working life in various industries. The latest generation of these coatings is the multilayer or hybrid type of nickel-phosphorus electroless coatings. In this research, for the first time, a three-layer Ni-P/Ni-P-Al_2O_3/Ni-P-SiC coating was produced and its tribological properties were investigated. X-ray diffraction test, energy beam spectrometer, optical and electron microscope images, hardness measurement, roughness measurement, adhesion test (according to ASTM B571 standard), and pin-on-disk wear (according to ASTM-G99 standard) were used for characterization. In the X-ray diffraction pattern related to the multilayer coating, in addition to the amorphous nickel-phosphorus phase, SiC and Al_2O_3 phases were also seen. The hardness of multilayer coating was 126 Vickers more than that of single-layer coating. The adhesion of all the coatings was very good, so after performing the bending test, no galling was observed in the coatings. In general, it was found that the use of multi-layer coating compared to single-layer coating (with the same thickness) leads to increased hardness, better adhesion, and superior wear behavior. The wear mechanism of the coatings was also evaluated with the help of electron microscope images and energy-dispersive X-ray spectroscopy. The wear mechanism of the electroless nickel-phosphorus coating was delamination and Abrasive, while the hybrid coating changed the mechanism to adhesive by creating a gradient of mechanical properties and lubrication.

Keywords: Multilayer Coating, Wear Mechanism, Adhesion, Nickel-Phosphorus.

1. Introduction

The properties required inside and on the surface of industrial parts may differ from each other. Inside, properties such as toughness, strength, creep resistance, and at the level of low friction coefficient, high wear resistance and appropriate corrosion behavior are important. Simultaneously achieving these properties by creating surface layers on engineering parts can make this challenging task possible. Electroless nickel-phosphorus coatings are one of the most widely used layers applied to parts made of different materials such as steel, due to their excellent surface properties and reasonable cost of production [1,2]. However, all electroless coatings do not show the same resistance to wear and corrosion. High phosphorus coatings provide excellent corrosion resistance, while low phosphorus or medium phosphorus coatings are not recommended for use in highly corrosive environments. On the other hand, coatings with low phosphorus have high hardness and high wear resistance. While increasing the amount of phosphorus, the hardness and wear resistance decreases. In recent years, multilayer coatings have received more attention because these types of coatings can significantly improve coating properties. For example, it is possible to create a hybrid coating whose hardness increases from the substrate to the surface. This prevents the concentration of stress at the interface between the substrate and the coating and can provide excellent resistance to crack growth and corrosion [3]. The middle layer that is applied on the substrate has the role of coating adhesion, while the upper layers provide anti-corrosion and anti-wear properties. Studies have shown that multilayer coatings are more effective in dealing with wear. Also, the use of SiC reinforcing particles such as TiO_2, B_4C, and ZrO_2 in one of the layers of these coatings has been able to create a very suitable tribological behavior.[1-3].

Wang et al. [4] investigated Ni-P-ZrO_2/Ni-P double-layer coatings applied by electroless method. The ability to improve wear properties with the help of produced concentration gradient as well as added composite particles was clearly evident in the results. The double-layer coating containing nickel-phosphorus/nickel-boron coating has been investigated, and the double-layer coatings have performed very well in the wear test, which is directly related to the lubrication properties of the double-layer coatings [5].

Hong et al. [6] investigated and characterized the Ni-P/Ni-W-P double-layer coating by electroless

*Corresponding author
Email address: mohamad.razazi@yahoo.com

method. The results indicated a significant increase in the wear resistance of the produced double-layer coating.

A study has been done by Wang et al. [7] on Ni/Ni-B-TiO_2 bilayer coatings. In this research, titanium oxide particles were trapped in the upper layer of the coating, which led to a significant increase in hardness and improved wear behavior of the electroless nickel-phosphorus coating.

Until now, the use of silicon carbide and aluminum oxide reinforcing particles in nickel-phosphorus electroless multilayer coating layers has not been studied, which will be evaluated for the first time in this research. Therefore, considering the extraordinary tribological properties that silicon carbide can create in composite coatings, this study can take a big step in reducing the destruction of engineering parts against wear.

2. Materials and Methods

In this research, plain carbon steel ST37 was used as the substrate. Before the coating process, sanding, polishing, and washing were done. Two types of single-layer and multi-layer (hybrid) coatings were chosen for the study. The single-layer coating was done by SLOTONIP 70A nickel-phosphorus electroless bath, made in Germany - Schlotter company, with a duration of 50 minutes. In the bath for the second and third stages, the basic solution was the same as SLOTONIP 70A, containing 10 g/l of SiC particles with a particle size below 5 microns and Al_2O_3 with a particle size of 2 to 15 microns, respectively. Analysis of surface morphology and chemical composition of coatings was done with the help of an optical microscope, scanning electron microscope, and Energy-Dispersive X-ray spectroscopy (EDS). Phase identification of the coatings was done by an X-ray diffraction analyzer. The microhardness of the coatings was checked with the help of the Koopa microhardness tester. The roughness of the specimens was checked with the help of a portable Mitutoyo device, which also showed the roughness graph by connecting to the computer and using the relevant software. To analyze the adhesion of single-layer and multi-layer coatings, the three-point flexural test was used according to the ASTM B571 standard. The way to perform this test is that the covered specimen is bent using a mandrel whose thickness is 4 times the thickness of the specimen until the two ends of the specimen become parallel. In this test, separation of the shell from the substrate means weak adhesion of the coating to the substrate. The wear test was performed by the pin-on-disk test according to the ASTM-G99 standard.

After the loadability test at the test temperature of 30°C, a load of 1.5 kg was selected as the wear load. The wear distance was considered to be 800 meters. Finally, in order to obtain the effective wear mechanisms in wear, SEM images and EDS analysis of the wear surfaces and also the particles removed during the test were prepared.

3. Results and Discussion

Fig. 1. shows optical microscope images of both Ni-P single-layer and Ni-P/Ni-P-Al_2O_3/Ni-P-SiC multilayer coatings. Both coatings have a dome-shaped or cauliflower-like structure, which is a characteristic of nickel-based electroless coating. By comparing the pictures, it can be pointed out that the dimensions of the domes are slightly smaller in the case of the composite coating, which is due to the type of precipitation mechanism in the electroless process. In the electroless process, the growth will be atom-by-atom regeneration. At first, nickel deposition is created in places with suitable surface energy, and then, with the availability of conditions and the stability of nickel buds, the growth of the coating will continue in these places.

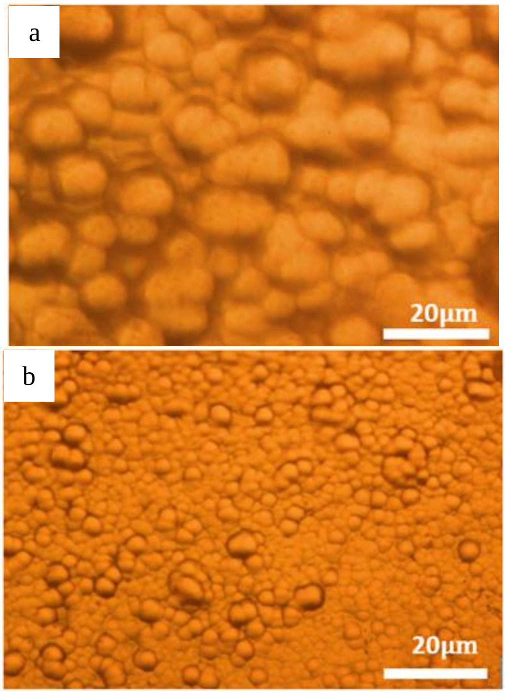

Fig. 1. Optical microscope images of the surface of a) single-layer coating and b) multilayer coating

In the case that the electroless solution was without composite particles, this nickel nucleation and deposit growth will continue up to high levels. However, when the solution has composite particles, during the deposition of the nickel-phosphorus coating, the particles are also absorbed in different places of the coating, and in a way, the composite settlement mechanism occurs with the process of being trapped throughout the deposited coating. Now, when the composite particles are placed on the nickel buds in some places, these places may not be suitable places to continue the growth process, and their surface energy may change [8].

Therefore, the growth will continue from the points very close or attached to the coating particles. With this process, the coating domes on the surface will be limited to growth and enlargement, although it is minor, and in addition to the surface energy, this issue will also be effective for the formation of the domes. For this reason, the surface domes of the composite coating are somewhat smaller than the conventional electroless nickel-phosphorus coating.
Fig. 2. shows the electron microscope images of the surface of both coatings. In this form, the surface domes fully express the quality of production coatings [9]. In the case of composite coating, a darker phase can be seen in some places, which is due to the presence of silicon carbide composite particles.

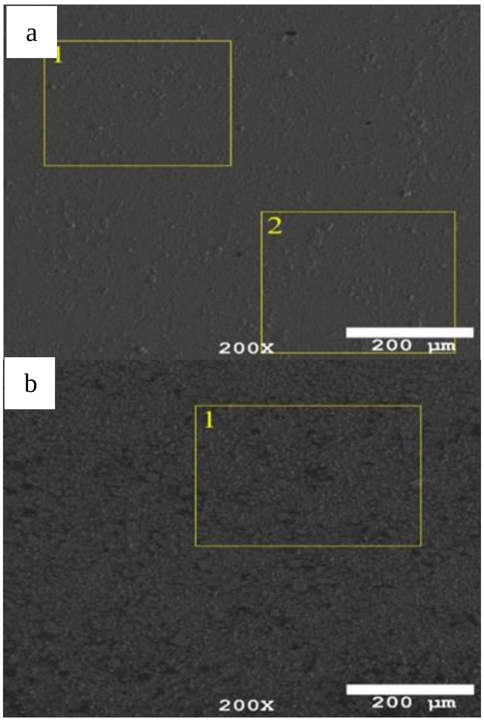

Fig. 2. SEM images of the surface of a) single-layer and b) multilayer coatings.

To prove this issue and to analyze the chemical composition of the coatings from different areas of their surface, EDS analysis was performed. The results of this test are presented in Table. 1. and Table. 2. According to these results, the normal nickel-phosphorus coating has 12.90 wt.% of phosphorus and the composite multilayer coating has 10.95 wt.% of phosphorus. In addition to nickel and phosphorus, carbon and silicon elements are also seen in the multi-layer composite coating, which indicates the presence of reinforcing particles. In the analysis with a more limited area related to the composite coating (Table. 2.), the amounts of silicon and carbon elements are significantly higher, which shows that these particles are definitely SiC particles (black dots).

Table. 1. EDS analysis results related to Fig. 2.a.

Element	Amount in wt.% in area 1	Amount in wt.% in area 2
Ni	87.100	87.370
P	12.900	12.630

Table. 2. EDS analysis results related to Fig. 2.b.

Element	Amount in wt.% in area 1	Amount in wt.% in area 2	Amount in wt.% in area 3
Ni	79.58	69.05	36.23
P	10.95	4.61	1.53
Si	7.16	19/79	42.08
C	2.31	6.55	20.16

In Fig. 3., the X-ray diffraction pattern of the coatings is drawn. Both coatings have a non-crystalline structure of nickel-phosphorus, which was predictable according to the articles according to the amount of phosphorus present in the coatings. The broad peak observed in the diffraction patterns that can be seen in both specimens can indicate three issues: First, the possible residual stress, which is due to severe mechanical operation in the specimen without annealing operation, and this phenomenon did not occur in this study. Secondly, due to the extreme thermal gradients and extreme thermal stresses remaining in the part, thermal stress is not created during electroless coating at all, and stirring operations will definitely prevent this from happening. On the other hand, thermal stress causes the broadening of the peak when there is melting and freezing, such as in the thermal spraying process. The nature of the electroless process is not melting and freezing [10]. Thirdly, it is due to the non-crystalline or amorphous structure of the coatings, in such a way that in the electroless process due to the high-speed settling of nickel atoms that turn into a solid state (if the conditions are ready) towards the substrate, sufficient permission is not given to be placed in preferred points in terms of crystal structure and the final coating will be non-crystalline and amorphous. No crystalline phase is observed in the typical electroless nickel-phosphorus coating (Figure 3-a), while in the multilayer composite coating, peaks of SiC and to a lesser extent Al_2O_3 were detected. SiC particles belong to the upper surface of the coating (third layer). It should be pointed out that if the coatings are porous, X-ray penetration will increase greatly, which cannot be justified considering the images taken from the surface of the specimens. In general, electroless coatings do not have much porosity and this issue is mentioned in the articles.
But again, it can be said that in the presence of reinforcing particles, there are gaps between the reinforcing particles and the nickel-phosphorus matrix, and it definitely helps the penetration of X-rays, even though it is small.

That is why, in the composite coating pattern (Fig. 2.b.), alumina, which was related to the bottom layers, has been identified. Despite the presence of elements other than nickel and phosphorus as well as phases such as SiC and Al_2O_3 in the composite coating, the final coating based on the amount of phosphorus is considered as a high phosphorus coating with a non-crystalline structure. It should be noted that for composite structures with high phosphorus, in some articles microcrystalline structures or metallic glass structures have also been mentioned [11].

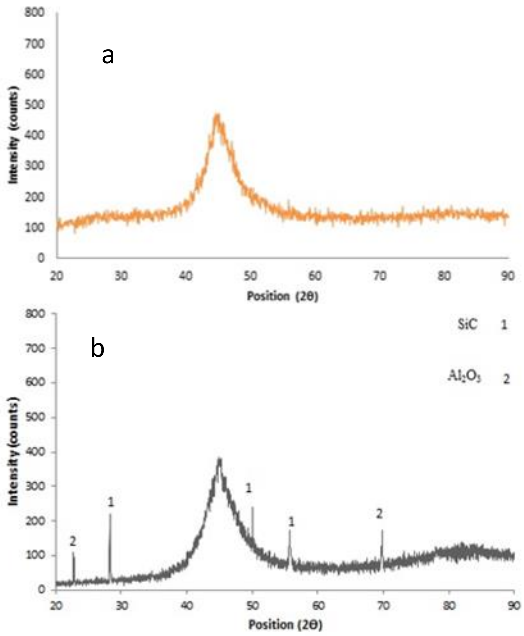

Fig. 3. XRD analysis results of a) single layer and b) multilayer coatings.

The hardness and roughness measurement results of the coatings are presented in Table. 3. It should be noted that the mentioned hardness is the average of 4 hardness testing times. Among these two specimens, the hardness of the multilayer coating is 126 Vickers, the main reason for which is the presence of hard reinforcing particles such as SiC on the surface of the coating.

Table. 3. The results of hardness measurement and surface roughness measurement of the specimens.

Specimen	Roughness (Micrometer)	Hardness (Vickers)
Single-Layer Coating	2.41±0.97	498 ±9
Multilayer Coating	1.80±0.62	624 ±21
Substratest37	0.19±0.26	122 ±11

Also, the presence of Al_2O_3 reinforcing particles in the lower layer will increase the overall ability of the surface to withstand the force of the hardness tester. It shows that this higher resistance leads to higher hardness. On the other hand, one of the most important features of hybrid coatings is the creation of a hardness gradient from the substrate to the surface of the coating, which can affect and increase the final hardness of the surface. For this purpose, in addition to the hardness of the coating surface, the hardness measurement was also performed from the cross-section of each layer, which is reported in Table. 4.

For the conventional coating, the hardness has increased by advancing from the substrate to the coating, but the hardness gradient has not been created except at the initial points of the coating attached to the substrate. However, in the multilayer coating, a complete hardness gradient is observed, which indicates the effect of SiC and Al_2O_3 reinforcing particles on the hardness of the nickel-phosphorus electroless coating. As can be seen in Table. 3. and Table. 4., the hardness of the coating in the Ni-P-SiC coating section is equal to 535 Vickers, while the final hardness of the multilayer coating that has a high level of Ni-P-SiC is 624 Vickers. This issue shows the influence of the harder bottom layers on the final hardness of the surface of multilayer coatings. Therefore, in general, it can be said that despite the non-crystalline or amorphous structure of the main phase of the matrix in both coatings, the placement of hard composite particles has increased the hardness of the multilayer coating.

Table. 4. Hardness measurement results of different sections of the coatings.

Place of hardness measurement	Hardness (Vickers)
Single layer Ni-P coating in conventional coating	465±12
Ni-P coating in multilayer coating	414±8
Ni-P-Al_2O_3 coating in multilayer coating	497±6
Ni-P-SiC coating in multilayer coating	535±10

As can be seen in Table. 3., the roughness of both coatings is close to each other, and the average roughness value of the multilayer coating is slightly higher. The reason for this difference can be analyzed from two perspectives:

i. According to the images obtained from the surface of the composite coating, the dimensions of the domes have been reduced in the presence of particles according to the mentioned explanations. In other words, multi-layer domes are less high. This incident has caused the intervals between the depressions and the protrusions of the multilayer coating to decrease. On the other hand, it can be said that if there is even a gap between the domes, these indentations increase with the help of the particles trapped between the domes, so the tip of the

roughness meter cannot enter the lower surface of the coating [12].
ii. An important feature of the electroless process is the ability to fill holes and distorted surfaces. When this process takes place in three stages, at the beginning of each stage, the filling of the holes begins, and with the settling of nickel deposits to higher levels, it becomes a dome and the roughness of cauliflower is formed. In fact, upon completion of the process in the first stage (the first layer of nickel-phosphorus), there is an unevenness that is filled with the second layer, and the third layer fills the unevenness with the second layer better. But in the single-layer coating, the process takes place without interruption, and the entire thickness is created continuously, allowing the growth of larger domes of electroless nickel-phosphorus deposits. Therefore, in the case of one-step coating, the final roughness is higher than that of multi-layer coating.
To determine the adhesive strength of the coatings, the bending test according to ASTM B571 standard was used. The basis of this test is macroscopic and microscopic. In the macro mode, if the coating does not have deep scratches after the test and the coating does not separate from the substrate, it means that the adhesion of the coating is acceptable. In Fig. 4., two images of both specimens can be seen, which shows that no separation has occurred for them and both have good adhesion.

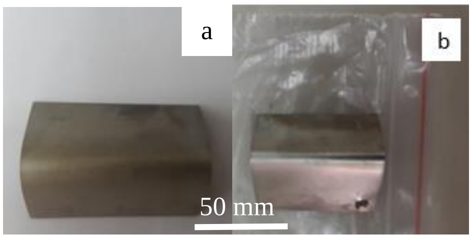

Fig. 4. Macro images of specimens after bending test a) single layer coating and b) multilayer coating.

According to this standard, microscopic images of the bending area should be prepared for more accurate comparison and analysis. This work was done, which these areas can be seen in Fig. 5. and Fig. 6. with different magnifications. The basis of the evaluation is the compression and density of the cracks, the maximum width of the crack and the distance between the cracks. The specimen with higher crack density, smaller crack width and smaller crack distance will have better adhesion. In other words, the smaller and more the cracks in the curved area, the better the adhesion. In both shapes, parallel cracks are observed for both specimens, but the multilayer coating has much better adhesion. Because in this coating, the number of cracks in this area is more, and the width of the cracks and the distance between the cracks are more. This issue, i.e. the better adhesion of the hybrid coating, has been proven in other studies in this field [13].

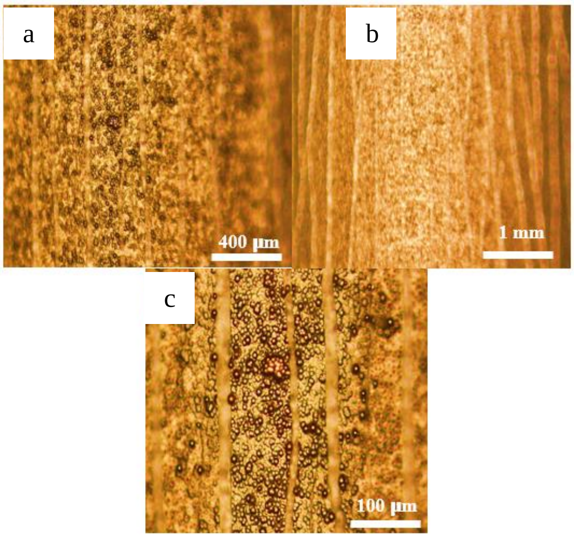

Fig. 5. Optical microscope images of the curved area of the single-layer coating after the bending test

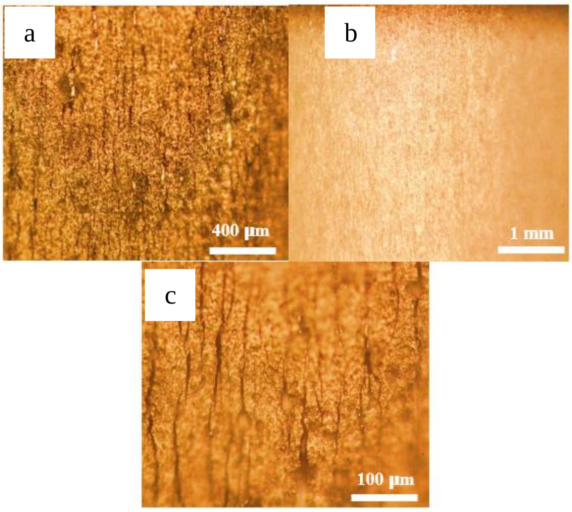

Fig. 6. Optical microscope images of the curved area of the multilayer coating after the bending test

Another important point that can be seen by comparing the images of Fig. 5. and Fig. 6. is that the pattern of cracks in the multilayer coating is fundamentally different from that of the single-layer coating, in such a way that the cracks are smaller, close to each other with different lengths and non-continuous. It can be seen in Fig. 6. that many cracks have stopped growing, and other cracks are starting to grow.
This issue indicates the concentration of low stress at the tips of the widened cracks in the multilayer coating. When the crack reaches even a small gap between the upper layer and the lower layer in the multilayer structure, the angle at the crack tip increases significantly. As a result, crack energy and stress concentration will decrease. During the bending test, tensile and compressive stresses are spread outside and inside the specimen under test, respectively [14].

In the multilayer specimen, the stresses are distributed in numerous interfaces of the upper and lower layers, and this uniform distribution leads to a reduction of the inappropriate stress level in the width and surface of the coating. Moreover, the decrease in the distance between the cracks is related to the shear stress introduced in the interfaces, and also, the density of the cracks is finally known as the basis of the adhesion strength [9], so because of these two reasons, the multilayer coating has a higher adhesion strength as seen in Fig. 6. Another effective factor is the presence of SiC reinforcing particles with favorable plastic properties, which by being present in the metal matrix has been able to improve the mechanical properties of the multilayer coating.

In order to investigate the tribological behavior of the coatings, the friction coefficient and weight reduction of the specimens were analyzed. The results related to the friction coefficient of the specimens are shown in Fig. 7. What is remarkable is the lower friction coefficient of both coatings compared to the substrate. This difference shows the excellent lubrication properties of nickel-phosphorus electroless coatings.

First, in electroless coatings, the dome-shaped topography can reduce the contact force between the surfaces (which causes changes in the friction coefficient) to a great extent, and somehow the self-lubricating property of electroless coatings depends a lot on this type of morphology [15]. Secondly, the presence of phosphorus, with the activation of appropriate sliding plates, allows more movement of the two bodies involved. On this basis, the presence of silicon carbide has been able to promote better lubrication of the entire multilayer coating. Finally, due to the higher hardness in the produced electroless coating, it does not allow the wear pin to enter more, and less frictional force is created between the surfaces.

The presence of SiC as a carbide with high hardness and good lubrication has been effective in further reducing the friction coefficient of the multilayer coating. Regarding the effect of the second layer containing Al_2O_3, it should be said that in the continuation of the wear path with the destruction of the upper layer of the coating, the appropriate hardness of the Ni-P-Al_2O_3 coating acts as an obstacle for further contact between the pin and the surfaces and has improved the frictional behavior of the multilayer coating.

The weight loss graph of the specimens is shown in Fig. 8., which shows that the multilayer coating had the highest wear resistance.

It seems that the two parameters of higher hardness and lower friction coefficient of the multilayer coating compared to the single-layer coating had the greatest effect on this wear resistance. On the other hand, the adhesion and deformability of the plastic specimen under test are of great importance.

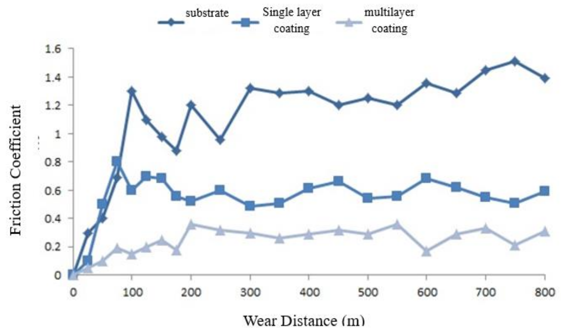

Fig.7. Changes in the friction coefficient of the specimens during the wear process.

As seen in the previous section, the multilayer coating had the best adhesion, which coincides with the ability to change the shape of plastic in the presence of silicon carbide particles, making this coating have a good tolerance against abrasive forces. In other words, the critical stress required to tear off the multilayer coating from the substrate is much higher than the single-layer coating, and therefore, the particles are broken or torn off under greater forces. It should be noted that the creation of the hardness gradient of bearing the stress resulting from the wear forces for multilayer coatings is also a factor that can affect the wear resistance

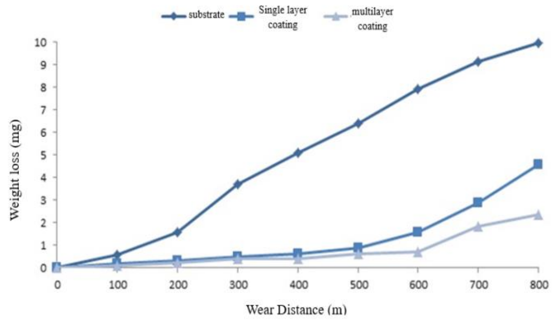

Fig.8. Graph of weight loss of specimens along the wear path.

In order to analyze the wear mechanism of the coatings, electron microscope images were prepared along with X-ray energy spectrogram analysis of wear surfaces. Fig. 9.a. shows the image of the single-layer coating. The first mode that can be seen in the destruction of the surfaces of this coating is the flaky and relatively deep model. In this case, the coating has been peeled from the surface in the form of sheets upon reaching the maximum tolerable stress, which indicates a sheet mechanism. Moreover, scratches in the direction of wear and one side are clearly visible, which indicates the abrasive mechanism. Conducting the EDS analysis of the surface of this coating (the results are reported in Table 5) shows that no trace of elements related to the pin can be seen, and this means the absence of an adhesive mechanism. Also, the oxygen element is not seen in the results of the analysis, so the claim of the existence of an oxidative wear mechanism is rejected [16]. In terms of dimensions, the debris resulting from wear (Fig. 9.b) shows that they are completely fragmented and large, which is in line with the influence of the dominant sheet mechanism in this specimen.

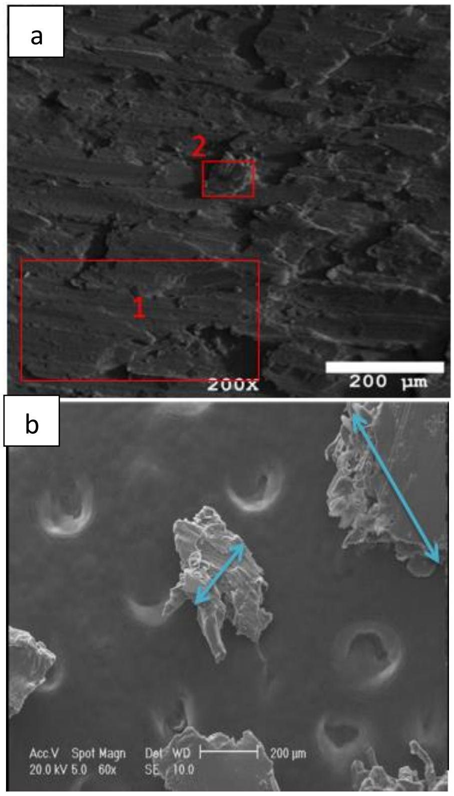

Fig. 9. Electron microscope images related to single-layer coating a) wear surface b) wear debris.

Table. 5. EDS analysis results related to Fig. 9.

Element	Amount in wt.% in area 1	Amount in wt.% in area 2
Ni	91.600	94.290
P	8.400	5.710

The wear surfaces of the multilayer coating (Fig. 10.a.) show that the amount of destruction is completely reduced and the depth of the surface loss is less in all places. On the other hand, there is almost no abrasive wear (parallel grooves in the direction of wear), which indicates better lubrication of this coating. EDS analysis of the center and sides of the surface shows (Table. 6.) that the iron element can be seen in the center, which proves the adhesion of the wear mechanism of the specimen.

Table. 6. EDS analysis results related to Fig. 10.

Element	Amount in wt.% in area 1	Amount in wt.% in area 2	Amount in wt.% in area 3
Ni	77.21	60.65	63.40
P	5.54	6.62	5.81
Si	3.02	31.71	27.48
Fe	14.23	1.02	3.31

The presence of silicon element with a greater amount in the areas next to the wear path than in the central areas of the wear surface also shows this, silicon carbide particles by being placed against the wear pin prevented further progress and as a result, the surface of the wear was less. The dimensions of the abrasion debris (Fig. 10.b) are also far less than the previous state, and it shows that the wear mechanism has been fully effective in the presence of reinforcing particles and the multi-layered coating. On the other hand, when the coating is a single layer, the peeling of the coating can be more because the interface is only between the coating and the substrate. While, for the hybrid coating, the force applied by the pin must first overcome the force of the interface between the upper coating and the lower coating, and then put the lower coating and finally the coating/substrate interface under tension. With the distribution of the tension that exists between the hybrid coatings, the volume of the material removed from the involved object will be less, which was fully observed in the images of the wear surface and the debris.

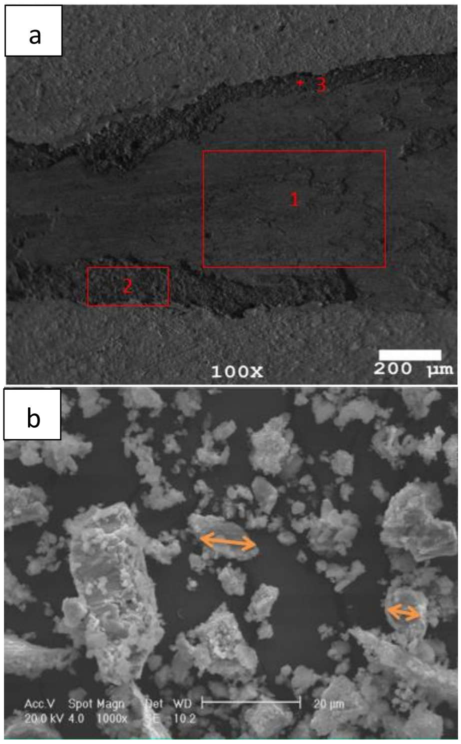

Fig. 10. Electron microscope images related to multilayer coating a) wear surface b) wear debris.

4. Conclusion

1. The phase structure of the single-layer coating was completely non-crystalline. In the XRD pattern related to the multilayer coating, in addition to the amorphous nickel-phosphorus phase, SiC and Al_2O_3 phases were also seen, which were related to the reinforcing particles in the different layers of the coating.

2. Single-layer and hybrid multilayer coatings both had a dome-shaped morphology, and the domes observed in the multilayer coating were smaller.
3. The adhesion of all the coatings was very good so after performing the bending test, no peeling was observed in the coatings.
4. Examining the curvature area after the bending test with the help of microscopic images indicated a much better adhesion of the multilayer coating due to the better toughness and better continuity of the layers.
5. The hardness of the multilayer coating was 126 Vickers more than the single-layer coating, which is related to the presence of hard ceramic phases such as silicon carbide in this hybrid coating.
6. The friction coefficient of the coatings was far less than the steel substrate, and the good lubrication of all the coatings was due to the presence of phosphorus and their dome topography.
7. The wear mechanism of the electroless nickel-phosphorus coating was delamination and abrasive, while the hybrid coating changed the mechanism to adhesive by creating a gradient of mechanical properties and lubrication.

References

[1] Kumar S, Banerjee T, Patel D. Tribological characteristics of electroless multilayer coating: a review. Mater.Today: proc. 2020; 33:5678-82.

[2] Fayyad EM, Abdullah AM, Hassan MK, Mohamed AM, Jarjoura G, Farhat Z. Recent advances in electroless-plated Ni-P and its composites for erosion and corrosion applications: a Rev. Emergent Mater. 2018; 1:3-24.

[3] Sudagar J, Lian J, Sha W. Electroless nickel, alloy, composite and nano coatings–A critical Rev. J. Alloys Compd. 2013; 571:183-204.

[4] Wang Y, Shu X, Wei S, Liu C, Gao W, Shakoor RA, Kahraman R. Duplex Ni–P–ZrO2/Ni–P electroless coating on stainless steel. J. Alloys Compd. 2015; 630:189-94,

[5] Vitry V, Bonin L. Formation and characterization of multilayers borohydride and hypophosphite reduced electroless nickel deposits. Electrochim. Acta. 2017; 243:7-17.

[6] Hong LI, Guo RX, Zhu LI. Characteristics of microstructure and performance of laser-treated electroless Ni–P/Ni–W–P duplex coatings. Trans. Nonferrous Met. Soc. China. 2012; 22(12):3012-20.

[7] Wang SJ, Wang Y, Shu X, Tay S, Gao W, Shakoor RA, Kahraman R, Preparation and property of duplex Ni–B–TiO_2/Ni nano-composite coatings. Int. J. Mod. Phys. B. 2015; 29(10n11):1540022.

[8] Yang Z, Xu H, Shi YL, Li MK, Huang Y, Li HL. The fabrication and corrosion behavior of electroless Ni–P-carbon nanotube composite coatings. Mater. Res. Bull. 2005; 40(6):1001-9.

[9] Mohanty S, Jamal N, Das AK, Prashanth KG. Electroless Ni-P-MoS_2-Al_2O_3 composite coating with hard and self-lubricating properties. Mater. 2022; 15(19):6806.

[10] Ranganatha S, Venkatesha TV, Vathsala K. Development of electroless Ni–Zn–P/nano-TiO_2 composite coatings and their properties. Appl. Surf. Sci. 2010; 256(24):7377-83,

[11] Shu X, He Z, Wang Y, Yin L. Mechanical properties of Ni-based coatings fabricated by electroless plating method. Surf Eng. 2020; 36(9):944-51.

[12] Singh G, Mohanty S, Singh RK, Dixit AR, Sharma AK. Comparative study on electroless composite coatings of textured and untextured Al-substrates. Mater. Today: Proc. 2023; 80:233-40.

[13] Murali P, Gopi R, Saravanan I, Devaraju A, Karthikeyan M. Wear and mechanical properties of electroless NiP and NiP-Silicon Carbide (SiC) composite coatings on En8 steel. Mater. Today: Proc. 2022; 68:1707-10.

[14] Wang Y, Guan L, He Z, Zhang S, Singh H, Hayat MD, Yao C. Influence of pretreatments on physicochemical properties of Ni-P coatings electrodeposited on aluminum alloy. Mater. Des. 2021; 197:109233.

[15] Ni M, Wang S, Huang W, Li W. A novel self-lubricating Ni-P-AlN-WS 2 nanocomposite coating. Mater. Res. Express. 2019; 6(11):116413.

[16] Cao J, Zhao W, Wang X, Zhao Y, Ma P, Jiang W, Song G. The microstructure and tribological behavior of ultrasonic electroless Ni-P plating on TC4 titanium alloy with heat-treatment. Ferroelectrics. 2022; 589(1):1-1.